Power-shifted microwave resonances of a hot cavity filled with a surface-ionized alkali-metal plasma: Theory and experiment

Kwang-Seok Kim* and Howard H. Brown, Jr.
Department of Physics, New York University, New York, New York 10003
(Received 5 February 1986)

A new kind of thermal plasma device has been constructed consisting of an indirectly heated 2100 K *X*-band microwave cavity. The cavity is filled with a surface ionized K or Cs plasma with densities of from 1×10^{16} to 1×10^{17} m^{-3}. As a first experiment, the frequency of the TM_{010} mode has been measured as a function of microwave power absorbed by the cavity. The measurements are carried out under conditions where instabilities are not observed in the plasma. The resonant frequency is found to decrease as the microwave power increases. Two theories are developed to explain the frequency shifts, one depending on the ponderomotive force, the other on high-frequency resistive electron heating. Frequency shifts predicted by the ponderomotive force theory are substantially smaller than the observed shifts. The data are in reasonable agreement with the resistive-electron-heating theory if it is assumed that the work function of the microwave cavity wall is decreased by alkali-metal-atom coverage.

I. INTRODUCTION

Surface ionized alkali plasmas confined in hot ($\sim$2100 K) refractory metal boxes have in the past been used to study transport and charged-particle energy-loss phenomena.[1–4] Until perturbed, these plasmas are spatially homogeneous away from the wall and aperture sheaths, and are in near thermodynamic equilibrium with the walls of the box. The electron and ion temperatures are equal and magnetic fields are negligible unless externally applied. A new version of this kind of plasma device has been constructed in which the confining box is a cylindrical x-band microwave cavity suspended from two refractory metal wave guides. The wave guides and cavity are coupled by narrow slits. Plasma densities are from 10^{16} to 10^{17} m^{-3} which correspond to plasma frequencies of from 0.9 to 2.8 GHz. The microwave frequency is 3—10 times the plasma frequency. Due to the low energy ($<\frac{1}{4}$ eV) of the unperturbed plasma particles and the Q of the cavity, modest microwave power (<10 W) will significantly perturb the plasma.

In the first experiment with this new device the frequency of the TM_{010} mode of the plasma-filled cavity is measured as a function of the microwave power into the cavity. The microwave power and particle densities are low enough so that ionization produced by the microwave power is negligible. At the highest microwave powers used, low-frequency oscillations are observed at some microwave frequencies. These conditions are avoided in the data presented. It is found that the resonant frequency moves downward as the microwave power increases. Two possible causes of the power shift are examined theoretically. One is the ponderomotive force, which pushes the plasma away from regions of high microwave field intensity and makes the resonant frequency tend toward the lower vacuum value as the microwave power is increased. The other is high-frequency resistive electron heating caused by the microwave power. It is shown that electron heating decreases the charged-particle density while increasing the neutral-atom density. Again, a downward shift in resonant frequency results. The calculated frequency shifts produced by the ponderomotive force are too small to account for the observed results. The calculated frequency shifts due to resistive electron heating are in good agreement with the data if the work function of the alkali-coated rhenium-plated cavity wall assumes values of from 4.60 to 4.81 eV, the lower value corresponding to higher alkali densities.

Section II is a brief description of the plasma and apparatus. Section III outlines a computer calculation of the shift in the resonant frequency of the TM_{010} mode due to ponderomotive force effects. The electron heating, the concomitant plasma-density changes, and the resulting frequency shifts are evaluated in Sec. IV. Section V describes the apparatus in more detail. Formulas used for determining the cavity power and Q are derived in Sec. VI. The experimental procedures and data are presented in Sec. VII, and the results are discussed in Sec. VIII. In the Appendix the frequency shift due to the ponderomotive force is calculated using perturbation theory. This is used as a check on the computer calculation.

II. THE PLASMA

In this section a description of the salient parts of the plasma device are given along with a few governing equations so that the following theory will be in context. More details of the apparatus appear in Sec. V. Figure 1 is a sketch, not to scale, of the plasma-filled microwave cavity, its wave-guide support, the alkali-feed system, and the surrounding coaxial heating element. The cylindrical Ta cavity is suspended from two Ta waveguides of standard x-band dimensions. The coupling is through slits. While the cavity can be operated in a microwave transmission mode, the data presented are taken using only one waveguide by the microwave-reflection method. An opti-

 ©1987 The American Physical Society

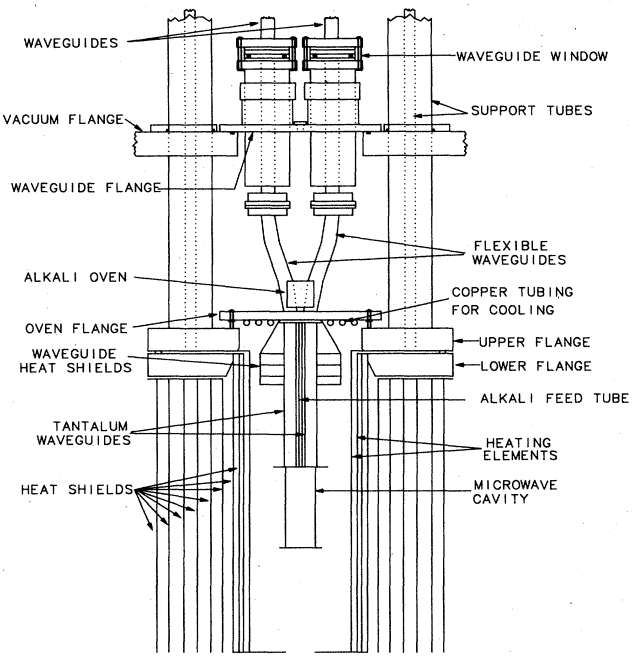

FIG. 1. Sketch of the apparatus, not to scale. Important dimensions are in Sec. V of the text.

cal pyrometer is focused through a small hole in the side of the cavity to measure the temperature. To make up for the small plasma loss through the holes an alkali oven feeds the plasma chamber through a Ta tube. The cavity and waveguide are radiatively heated by a surrounding ohmic element. This element is coaxial so as to reduce the magnetic field at the cavity to ~ 1 G. The plasma chamber and heating element are surrounded by a number of Ta heat shields. This plasma device is contained in a large stainless steel high vacuum chamber.

When the microwave power is $\lesssim 10$ mW, which we designate as "low," the plasma parameters are essentially the same as with the microwave power off. Then the electron temperature T_e and the ion temperature T_i are both equal to the cavity-wall temperature T_w. With low microwave power, the plasma density and neutral particle density are denoted by n_{p0} and n_{n0}, respectively. We assume that n_{p0} and n_{n0} do not depend on position, an excellent approximation for this type of plasma. With the particles very close to thermodynamic equilibrium with the cavity walls, the densities and temperatures are related by the Saha equation, which for alkalis is

$$\frac{n_{p0}^2}{n_{n0}} = (2\pi m k T_w h^{-2})^{3/2} \exp[-(eI)/(kT_w)] \ . \tag{1}$$

I is the ionization energy of the atoms in eV, m is the electron mass, k is Boltzmann's constant, h is Planck's constant, and e is the electronic charge. For the parameters of the plasma and the dimensions of the cavity, the electron and ion temperatures are maintained mostly by collisions with the walls rather than by collisions between particles.

With the microwave power low, let the plasma frequency in rad/s with $\omega_{p0}=2\pi f_{p0}=[(n_{p0}e^2)/(\epsilon_0 m)]^{1/2}$, the resonant frequency of the empty cavity for the mode used be $\omega_0=2\pi f_0$, and the resonant frequency of the uniformly filled cavity be $\omega=2\pi f$. ϵ_0 is the vacuum permittivity. Using the cold plasma dielectric function K, where

$$K = 1 - \frac{\omega_{p0}^2}{\omega^2} = 1 - \frac{f_{p0}^2}{f^2} \ , \tag{2}$$

it follows that

$$\omega^2 = \omega_0^2 + \omega_{p0}^2 \ , \tag{3}$$

and

$$f^2 = f_0^2 + f_{p0}^2 \ . \tag{4}$$

With the microwave power high, where "high" means high enough to measurably alter the plasma parameters, the cavity will be uniformly filled if electron heating dominates over ponderomotive force effects. For this case let n_p and n_n be the plasma and neutral densities, let the plasma frequency be $\omega_p=2\pi f_p=[(n_p e^2)/(\epsilon_0 m)]^{1/2}$, and let the resonant frequency of the mode used be $\Omega=2\pi F$. Then

$$\Omega^2 = \omega_0^2 + \omega_p^2 \ , \tag{5}$$

and

$$F^2 = f_0^2 + f_p^2 \ . \tag{6}$$

If the microwave power is high and ponderomotive force effects dominate, the simple relations Eqs. (3)—(6) do not apply. The plasma density is nonuniform and solving for the eigenfrequencies is a nonlinear problem. This is addressed in Sec. III.

III. CALCULATION OF THE RESONANT FREQUENCY SHIFT DUE TO THE PONDEROMOTIVE FORCE

The TM_{010} cylindrical cavity mode is used in this work. Assume the cavity is filled with a fixed number of singly charged positive ions and electrons whose number is each $n_{p0}V$, where V is the volume of the cavity. Let E be the peak values of the sinusoidally varying electric field. When $E \neq 0$, the ponderomotive force pushes the electrons away from regions where E is high and the ions follow. The resonant frequency is reduced and tends toward the vacuum value ω_0 as E increases. The ponderomotive force on a single electron can be described by a quasipotential[5] which can be used, along with the momentum equations for the ions and electrons, to give the electron plasma density $n_p(r)$ as

$$n_p(r) = n_{pw} \exp[-(eE)^2/(8m\omega^2 k T_e)] \ , \tag{7}$$

where n_{pw} is the electron density at the cylindrical wall where $E=0$. Note that $n_p(r)$ is the plasma density in the presence of the microwave field, and n_{p0} is the plasma density when the microwave power is off. The derivation of Eq. (7) assumes that $T_e=T_i$ and that neither T_e nor T_i depends on position. $n_p(r)$ depends on position through the spatial dependence of E. The dielectric function can

now be written as

$$K=1-\frac{e^2 n_{pw}\exp[-(eE)^2/(8m\omega^2 kT_e)]}{\epsilon_0\omega^2 m} . \quad (8)$$

The resonant frequency of the plasma-filled cavity with $E\neq 0$ has been obtained by a self-consistent numerical calculation patterned after that used by Motz.[6,7] Although the TM_{010} mode has only a radial dependence, the calculation is set up to include axial variations for use in future work. Assuming an $\exp(i\omega t)$ time dependence, Maxwell's equations are written as

$$\nabla\times\mathbf{E}=-i\omega\mu_0\mathbf{H} , \quad (9)$$

and

$$\nabla\times\mathbf{H}=i\omega\epsilon_0 K\mathbf{E}=i\omega\epsilon_0\left[1-\frac{n_p(r)e^2}{\epsilon_0\omega^2 m}\right]\mathbf{E} . \quad (10)$$

$\mathbf{H}$ is the magnetic intensity, μ_0 is the vacuum permeability, and $n_p(r)$ is given by Eq. (7). Letting r, θ, and z be the cylindrical coordinates, we note that $H_z=0$ and $\partial/\partial\theta=0$. If the radial and axial parts of Eq. (10) are substituted into the azimuthal part of Eq. (9), the result is

$$\frac{1}{r}\frac{\partial}{\partial z}\left[\frac{1}{K}\frac{\partial\phi}{\partial z}\right]+\frac{\partial}{\partial r}\left[\frac{1}{Kr}\frac{\partial\phi}{\partial z}\right]+\frac{\omega^2\phi}{c^2 r}=0 , \quad (11)$$

where $\phi=rH_\theta$. Equation (11) plus the boundary conditions define a nonlinear eigenvalue problem whose eigenvalues yield the resonant frequencies, and whose eigensolutions the magnetic field. The boundary conditions are $\phi=0$ on the axis, $\partial\phi/\partial z=0$ everywhere, and $\partial\phi/\partial r=0$ at $r=a$, where a is the cavity radius. The last boundary condition follows from $E_z=0$ at $r=a$. K is a function of r through the dependence of $n_p(r)$ on E.

Equation (11) is solved by a double-iteration method consisting of an "inner" and "outer" iteration. A radius of the cavity is divided into a mesh of up to 100 segments. The derivatives in Eq. (11) are replaced by central finite differences, and the resulting difference equations are cast in matrix form. If the mesh-point values of K are specified, the lowest eigenvalue and corresponding eigenvector are obtained by the inner iteration.[8] The eigenvalue gives the mode frequency and the components of the eigenvector the value of H_θ at the mesh points. The corresponding values of E at the meshpoints are obtained by using Maxwell's equations.

The resonant frequency and fields of the plasma-filled cavity containing a given number of plasma particles and a given electromagnetic energy are calculated as follows. First K is set equal to the vacuum value of 1 in the differences equations that represent Eq. (11), and arbitrary values of H_θ are assumed at the mesh points. The inner iteration, consisting of calculating the eigenfrequency and eigenfields, is then performed. When the inner iteration produces no more change in H_θ, the spatial dependence of E is calculated from Maxwell's equations. The fields obtained agree with the analytic values. With the spatial dependence of the vacuum fields known, they are normalized so as to agree with the microwave power delivered to the cavity and the Q of the cavity. The relative values of $n_p(r)$ at the mesh points are then calculated from Eq. (7),

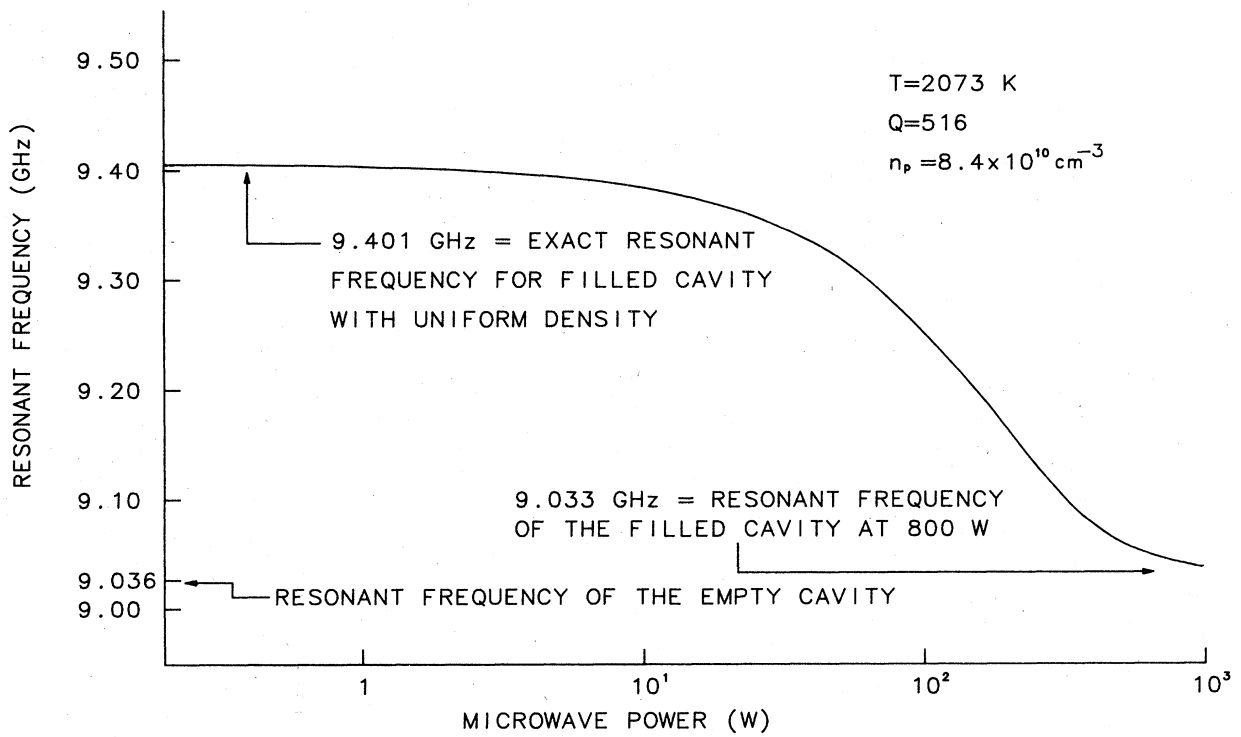

FIG. 2. Resonant frequency vs the microwave power absorbed by the cavity as predicted by the ponderomotive force theory.

after which $n_p(r)$ is normalized to give the assumed number of plasma particles in the cavity. The values of the density along with the vacuum resonant frequency are used to calculate K at the mesh points. The inner iteration is used again to calculate a new eigenfrequency and the unnormalized eigenfields. The outer iteration, consisting of normalizing the new fields, calculating the spatial dependence and normalization of $n_p(r)$, and using $n_p(r)$ and the new eigenfrequency to calculate K, is then executed. The inner iteration is then performed again. Both the inner and outer iterations are repeated until successive values of the eigenfrequency differ by less than 1 MHz.

An example of the computer-generated resonant frequencies as a function of the microwave power absorbed by the cavity is shown in Fig. 2 for a cavity Q of 516. The constant plasma temperature is 2073 K and the uniform density at low power is $n_{p0}=8.4\times10^{16}$ m^{-3}. For no microwave power in the cavity, the analytically calculated resonant frequencies are 9.401 GHz for the filled cavity and 9.036 GHz for the empty cavity. These frequencies are shown in the figure. The computer-generated frequencies should tend toward the former at low power and the latter at high power. This is indeed the case and is one check on the computer results. Figure 3 shows the spatial variation of the plasma density as a function of distance from the cavity axis for microwave powers from 0.05 to 20.0 W. Clearly shown in this figure is the movement of plasma from high-field regions to low-field regions. An interesting feature is that the curves intersect at a single point. This is also true for other temperatures and densities. This fact may be due to a peculiarity of the TM_{010} mode; the electric field is everywhere perpendicular to the gradients in the electric field and the gradients produced in the plasma density. To the accuracy of the computer calculation, this results in an electric-field configuration that is independent of the microwave power. This is verified by the computer calculations. Figure 4 shows the computed electric field versus cavity radius for a number of microwave powers. If the curves are normalized at one radius, they fall on top of one another.

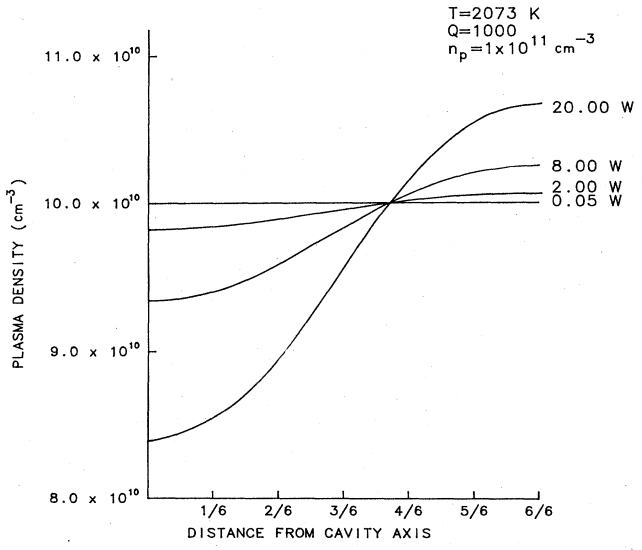

FIG. 3. Spatial dependence of the plasma density as predicted by the ponderomotive-force theory for various microwave powers absorbed by the cavity. The distance from the cavity axis is given as the fraction of the cavity radius.

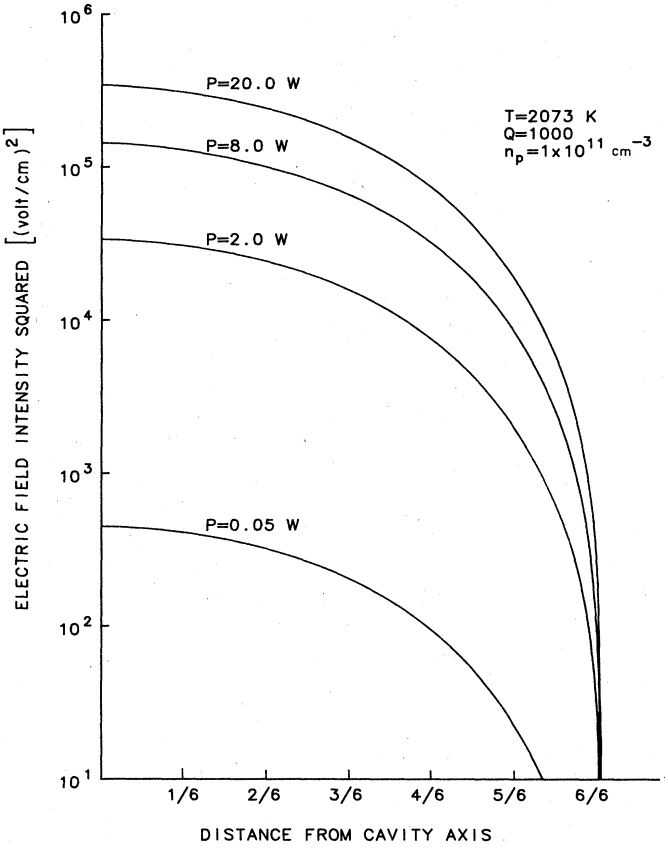

FIG. 4. Square of the electric field intensity vs the distance from the cavity axis. The distance from the cavity axis is given as the fraction of the cavity radius.

IV. ELECTRON HEATING EFFECTS

With the densities and temperatures used in this experiment, the flux density of electrons from the plasma toward the cavity wall sheath is always greater than the thermionic-emission flux density of electrons from the wall into the wall sheath. Steady-state conditions then require that the sheath potential ψ be such that the plasma is positive with respect to the wall. Then most of the electrons when they enter the sheath from the plasma are repelled back out without having hit the wall, and are in poor thermal contact with the wall. On the other hand, the ions, once having entered the sheath, will practically always hit the wall and are in good thermal contact with the wall. As a result of the weak electron-wall interaction, the strong ion-wall interaction, and the weak electron-ion interaction, modest microwave power will heat the electrons so that $T_e > T_i$, but T_i will remain close to T_w.

As the electrons get hot, it will be shown that the number of electrons and ions in the cavity decreases and the

neutral density increases. This lowers the resonant frequencies of the cavity, an effect we calculate as follows. The electron flux density from the plasma that hits the wall, Γ_e^{pw}, is given by

$$\Gamma_e^{pw}=\tfrac{1}{4}n_p\bar{v}_e\exp[-(e\psi)/(kT_e)]$$
$$=n_p\left[\frac{k\alpha_e T_w}{2\pi m}\right]^{1/2}\exp[-(e\psi)/(k\alpha_e T_w)]\ , \qquad (12)$$

where $\bar{v}_e=[(8k\alpha_e T_w)/(\pi m)]^{1/2}$ is the average electron speed in the plasma and $\alpha_e=T_e/T_w$. The exponential factor gives the fraction of the electrons incident on the sheath that surmount the sheath potential ψ and hit the wall. The electron flux density from the wall that enters the plasma, Γ_e^{wp}, is given by the Richardson equation as

$$\Gamma_e^{wp}=4\pi mk^2h^{-3}T_w^2\exp[-(e\varphi)/(kT_w)]\ , \qquad (13)$$

where φ is the work function of the wall. In steady state, $\Gamma_e^{pw}=\Gamma_e^{wp}$, leading to

$$n_p\left[\frac{k\alpha_e T_w}{2\pi m}\right]^{1/2}\exp[-(e\psi)/(k\alpha_e T_w)]$$
$$=4\pi mk^2h^{-3}T_w^2\exp[-(e\varphi)/(kT_w)]\ . \qquad (14)$$

The flux densities of ions and neutrals from the plasma to the wall, Γ_i^{pw} and Γ_n^{pw}, respectively, are given by

$$\Gamma_i^{pw}=\tfrac{1}{4}n_p\bar{v}_i=n_p\left[\frac{k\alpha_i T_w}{2\pi M}\right]^{1/2} \qquad (15)$$

and

$$\Gamma_n^{pw}=\tfrac{1}{4}n_n\bar{v}_n=n_n\left[\frac{kT_w}{2\pi M}\right]^{1/2}\ . \qquad (16)$$

$\bar{v}_i=[(8k\alpha_i T_w)/(\pi M)]^{1/2}$ is the average ion speed, $\bar{v}_n=[(8kT_w)/(\pi M)]^{1/2}$ is the average neutral speed, and $\alpha_i=T_i/T_w$. M is the neutral or ion mass, and the neutrals are assumed to be at the wall temperature T_w. The flux of ions from the wall to the plasma. Γ_i^{wp}, is more complicated. The usual assumption made for thermal ions or neutrals hitting a hot metal wall is that the probability of leaving the wall as an ion P_i, is the same for both. P_i for alkalis is given by[9]

$$P_i=\{1+2\exp[e(I-\varphi)/(kT_W)]\}^{-1}\ . \qquad (17)$$

If the particle leaves as a neutral, it immediately reenters the plasma. If it leaves as an ion, it has a probability of $\exp[-(e\psi)/(kT_w)]$ of surmounting the sheath barrier and reentering the plasma, and a probability of $1-\exp[-(e\psi)/(kT_W)]$ of being repelled by the sheath and rehitting the wall. An incident ion or neutral from the plasma that hits the wall and comes off the wall as an ion could hit the wall as an ion a large number of times before coming off as a neutral or as an ion with enough energy to overcome the sheath barrier. The probability that a neutral or ion from the plasma (as distinguished from the sheath) hits the wall (first bounce) and comes off as an ion that enters the plasma is $P_i\exp[-(e\psi)/(kT_w)]$. The probability that the same neutral or ion hit the wall twice and be returned to the plasma as an ion is $P_i^2\{1-\exp[-(e\psi)/(kT_w)]\}\exp[-(e\psi)/(kT_w)]$, and that it hit the wall a third time and be returned as an ion is $P_i^3\{1-\exp[-(e\psi)/(kT_w)]\}^2\exp[-(e\psi)/(kT_w)]$. These terms represent the first three terms of an infinite geometric series that summed gives for F_i the fraction of incident ions or neutrals from the plasma that hit the wall and are returned to the plasma as ions,

$$F_i=\frac{P_i\exp[-(e\psi)/(kT_w)]}{1-P_i\{1-\exp[-(e\psi)/(kT_w)]\}}\ . \qquad (18)$$

From the above we now have

$$\Gamma_i^{wp}=(\Gamma_i^{pw}+\Gamma_n^{pw})F_i$$
$$=(\alpha_i^{1/2}n_p+n_n)\left[\frac{kT_w}{2\pi M}\right]^{1/2}F_i\ . \qquad (19)$$

Equating Γ_i^{pw} to Γ_i^{wp}, and using Eqs. (17) and (18) for F_i and P_i,

$$\frac{n_n}{n_p}=2\alpha_i^{1/2}\exp[e(I+\psi-\varphi)/(kT_w)]\ . \qquad (20)$$

Equating the neutral flux densities between plasma and wall gives the same equation. The plasma potential ψ can be eliminated between Eqs. (14) and (20), yielding the "modified" Saha equation

$$\frac{[n_p]^{\alpha_e+1}}{n_n}=\left[\frac{[2]^{\alpha_e-1}}{\alpha_i^{1/2}[\alpha_e]^{\alpha_e/2}}\right]\left[\frac{2\pi mkT_w}{h^2}\right]^{(3\alpha_e)/2}$$
$$\times\exp\{-e[I+(\alpha_e-1)\varphi]/(kT_w)\}\ . \qquad (21)$$

When the microwave power is low, n_p becomes n_{p0}, n_n becomes n_{n0}, and $\alpha_e=\alpha_i=1$. Equation (21) then reduces to Eq. (1), the usual Saha equation. The right-hand side of Eq. (21) has the factor $\exp\{[-e(\alpha_e-1)\varphi]/[kT_w]\}$ which makes the plasma density a sensitive function of the electron temperature $T_e=\alpha_e T_w$.

The microwaves heat the plasma electrons by delivering a power P_e to them. The electrons can lose energy by collisions with neutrals or ions, or by collisions with the cavity walls. For the plasma being studied, the last effect dominates. Let P_w be the net power exchange between the plasma and the wall due to electron flow. In steady state, $P_e=P_w$. First we calculate P_e. From page 324 of Shkarofsky, Johnston, and Bachynski,[10] the complex ac plasma electric conductivity σ is

$$\sigma=\frac{n_pe^2(\nu-i\omega)}{m(\nu^2+\omega^2)}\ , \qquad (22)$$

where ν is the electron-ion collision frequency. We assume ponderomotive forces are small enough so the n_p can be taken as independent of position. The computer calculation of Sec. III supports this. The real part σ_r of σ is $\sigma_r\cong(n_pe^2\nu)/(m\omega^2)$, where $(\nu^2+\omega^2)$ has been approximated by ω^2. The microwave power absorbed per unit volume by the plasma electrons ρ is

$$\rho=\tfrac{1}{2}\sigma_rE^2=\frac{n_pe^2\nu E^2}{2m\omega^2}\ , \qquad (23)$$

where, as before, E is the peak value of the electric field. From page 325 of Ref. 10, ν is obtained from $\nu=\Upsilon\ln\Lambda$, where

$$\Upsilon=\frac{n_p}{12}\left[\frac{2\pi}{m}\right]^{1/2}\left[\frac{e^2}{\pi\epsilon_0}\right]^2\frac{1}{(k\alpha_e T_w)^{3/2}} . \tag{24}$$

For Λ, the Debye length divided by the 90° impact parameter, the high-frequency form given by Eq. (7-29e) of Ref. 10 is used. This is

$$\Lambda=\frac{4\epsilon_0 m}{\zeta e^2 f}\left[\frac{2k\alpha_e T_w}{\zeta m}\right]^{3/2} , \tag{25}$$

where $\zeta=\exp(\gamma)$, and γ is Euler's constant. The total microwave power absorbed by the electrons P_e is

$$P_e=\int_V \rho\, d^3x=\frac{n_p e^2\nu}{2m\omega^2}\int_V E^2 d^3x , \tag{26}$$

where the integration is over the volume V of the cavity. Let the internal Q of the cavity be Q_0 (see sec. VI). From the definition of Q_0 and using the cold plasma dielectric function from Eq. (2), the integral in Eq. (26) can be expressed in terms of the microwave power absorbed by the cavity P_c as

$$\int_V E^2 d^3x=\frac{P_c Q_0}{\epsilon_0\pi f(1-f_p^2/f^2)} . \tag{27}$$

Combining Eqs. (23)–(27), the microwave power delivered to the plasma electrons is

$$P_e=\frac{P_c Q_0 n_p^2 e^6}{3(2\pi)^{9/2}(mk\alpha_e T_w)^{3/2}\epsilon_0^3 f(f^2-f_p^2)} \times\ln\left[\frac{2^{7/2}\epsilon_0(k\alpha_e T_w)^{3/2}}{e^2 m^{1/2}\zeta^{5/2} f}\right] . \tag{28}$$

For the calculation of P_w, let P_e^{pw} be the power due to electrons flowing from the plasma to the wall. If the z axis is normal to the wall, and if v_x, v_y, and v_z represent the Cartesian components of the electron velocities, then

$$P_e^{pw}=S\int_{v_x=-\infty}^{v_x=+\infty}\int_{v_y=-\infty}^{v_y=+\infty}\int_{v_z=(2e\psi/m)^{1/2}}^{v_z=+\infty} v_z n_p f(v)\tfrac{1}{2}m(v_x^2+v_y^2+v_z^2)dv_x\,dv_y\,dv_z , \tag{29}$$

where S is the area of the wall and $f(v)$ is the electron velocity distribution. Using the Maxwellian distribution for $f(v)$,

$$P_e^{wp}=Sn_p(e\psi+2k\alpha_e T_w)\left[\frac{k\alpha_e T_w}{2\pi m}\right]^{1/2}\exp[-(e\psi)/(k\alpha_e T_w)] . \tag{30}$$

Using Eq. (14) the exponential factor with ψ may be replaced with one containing φ, giving

$$P_e^{pw}=S4\pi mh^{-3}(kT_w)^2(e\psi+2k\alpha_e T_w)\exp[-(e\varphi)/(kT_w)] . \tag{31}$$

To calculate P_e^{wp}, the power delivered to the plasma by the thermionic wall electrons, the Fermi-Dirac distribution of the electrons in a metal $f_F(v)$ is used where

$$f_F(v)=2m^3h^{-3}\{1+\exp[e(\epsilon-\epsilon_F)/(kT_w)]\}^{-1}\cong 2m^3h^{-3}\exp[-e(\epsilon-\epsilon_F)/(kT_w)] . \tag{32}$$

Here ϵ is the electron kinetic energy and ϵ_F is the Fermi energy. As usual, we neglect the 1 in the denominator. Then again taking the z coordinate normal to the wall,

$$\begin{aligned}P_e^{wp}&=S\int_{v_x=-\infty}^{v_x=+\infty}\int_{v_y=-\infty}^{v_y=+\infty}\int_{v_z=v_L}^{v_z=+\infty} f_F(v)v_z[\tfrac{1}{2}m(v_x^2+v_y^2+v_z^2)+e(\psi-\epsilon_F-\varphi)]dv_x dv_y dv_z\\ &=S4\pi mh^{-3}(kT_w)^2(e\psi+2kT_w)\exp[-(e\varphi)/(kT_w)] ,\end{aligned} \tag{33}$$

where $v_L=\{[2e(\epsilon_F+\varphi)]/(m)\}^{1/2}$. The net power to the wall, P_w, is then

$$\begin{aligned}P_w&=P_e^{pw}-P_e^{wp}\\ &=8\pi Smh^{-3}k^3T_w^3(\alpha_e-1)\exp[-(e\varphi)/(kT_w)] .\end{aligned} \tag{34}$$

Letting $P_e=P_w$,

$$\frac{P_c Q_0 n_p^2 e^6}{3(2\pi)^{9/2}(mk\alpha_e T_w)^{3/2}\epsilon_0^3 f(f^2-f_p^2)} \times\ln\left[\frac{2^{7/2}\epsilon_0(k\alpha_e T_w)^{3/2}}{e^2 m^{1/2}\zeta^{5/2} f}\right] =8\pi Smh^{-3}k^3T_w^3(\alpha_e-1)\exp[-(e\varphi)/(kT_w)] . \tag{35}$$

The additional equations necessary to solve for the frequency shift due to electron heating are the following. Denote the sum of the ion and neutral densities by n_t, which is assumed independent of microwave power. With the microwave low,

$$n_t=n_{p0}+n_{n0} . \tag{36}$$

With the microwave power high,

$$n_t=n_p+n_n . \tag{37}$$

Equations (4) and (6) are written in terms of the plasma densities as

$$f^2=f_0^2+\frac{n_{p0}e^2}{\epsilon_0 m\,4\pi^2} \tag{38}$$

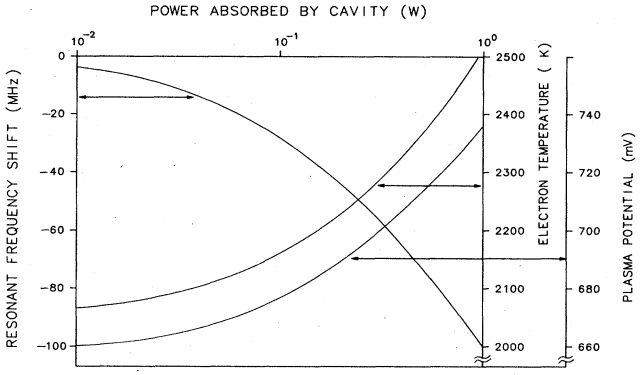

FIG. 5. Resonant frequency shift, electron temperature, and plasma potential as a function of the microwave power absorbed by the cavity. Plasma parameters are $n_{p0}=6.71\times10^{16}$ m^{-3}, $T_e=2048$ K, $Q_0=1751$, $\varphi=4.65$ eV, $f=9.345\times10^9$ Hz, and $f_0=9.051\times10^9$ Hz.

and

$$F^2=f_0^2+\frac{n_p e^2}{\epsilon_0 m\, 4\pi^2}\ . \tag{39}$$

Equations (35)—(39) together with the modified Saha relation Eq. (21) are sufficient to solve for the frequency shift $\Delta f=f-F$ if α_i is set equal to 1 in Eq. (21). This last assumption is justified by a calculation that shows that the ions do not get enough energy from the electrons to significantly raise their temperature. The following procedure is used to solve these six equations. It is assumed that T_w, f, f_0, I, φ, and Q_0 are known. T_w, f, f_0, and Q_0 are the quantities actually measured at very low microwave power. Equation (38) is used to obtain n_{p0}, and Eq. (1), which is Eq. (21) with $\alpha_i=\alpha_e=1$, is used to get n_{n0}. Equation (36) is then used to calculate n_t. Δf is specified, so that Eq. (39) can yield n_p, and n_n is obtained from Eq. (37). Equation (21) is solved for α_e, using the solve routine of a Hewlett Packard 15C calculator, and finally P_c is given by Eq. (35). By specifying various Δf's, a curve of frequency shift versus P_c is obtained.

Figure 5 shows three predictions of the hot-electron theory. The resonant frequency shift ($f-F$), the electron temperature T_e, and the plasma potential relative to the wall ψ are plotted as a function of the microwave power absorbed by the cavity, P_c. The plasma parameters are those of run No. 1: $n_{p0}=6.71\times10^{16}$ m^{-3}, $T_e=2048$ K, $Q_0=1751$, $\varphi=4.65$ eV, $f=9.345\times10^9$ Hz, and $f_0=9.051\times10^9$ Hz. One watt of absorbed microwave power decreases the resonant frequency by 100 MHz, raises the electron temperature to 2500 K, and raises the plasma potential from 656 and 735 mV. As the electron temperature increases, an increase in plasma potential is necessary to keep the net electron flux between plasma and wall zero. Additional curves of frequency shift versus microwave power appear in the data graphs of Sec. VII.

V. APPARATUS

Figure 1 shows the part of the apparatus that is inside a stainless steel high vacuum chamber. The plasma chamber is a cylindrical x-band microwave cavity which when cold has an inside diameter of 2.54 cm and a height of 8.052 cm. The cylindrical walls are 50.8-μm Ta foil and the ends 0.508-mm Ta sheet. The cavity is Re plated[11] to increase the surface ionization efficiency for alkalis hitting the surface. An optical pyrometer is sighted through a 0.794-mm hole in the cavity wall to measure the temperature. The cavity is suspended from two 1.016×2.286 cm rectangular Ta waveguides which are 17.1-cm long. The Ta waveguides have axial slots in the middle of the 2.286-cm sides for vacuum pumpout. The slots are positioned so as not to interfere with the TE_{10} waveguide mode. Only one of the waveguides is coupled to the cavity, a 0.508×11.43 mm coupling slit being used. The waveguides are attached to a stainless steel circular "oven" flange which is water cooled by Cu tubing. Above the oven flange two flexible sections of commercial Cu-Be x-band waveguide are attached. These are connected to straight waveguide sections which pass through the waveguide flange, after which they are sealed off by three iris resonant-type windows. The waveguide flange rests on top of the vacuum flange that seals off the top of the main vacuum chamber. An alkali oven sits on the oven flange and feeds alkali vapor to the cavity through a 3.175-mm-i.d. Ta tube. The oven flange rests on a pair of flanges designated as "upper" and "lower." These are water cooled, electrically insulated from each other, and held by a pair of coaxial support tubes that carry electric current and water to them. These two support tubes pass through and are mechanically connected to the vacuum flange. An Ohmic heating element surrounds the plasma chamber which it heats by radiation. This coaxial heating element is made from 25.4-μm W foil and consists of an inner cylinder and outer cylinder with diameters of 6.985 and 9.208 cm. The lower ends of the heating-element cylinders are connected together and the upper ends are attached to the upper and lower flanges which supply 480 A of regulated dc current. The coaxial design of the heating element and support tubes minimizes the magnetic field due to the heating current at the position of the microwave cavity. A large number of heat shields made from 25.4-μm Ta foil are shown in Fig. 1. After outgassing, the pressure in the vacuum chamber is $\sim1\times10^{-6}$ Torr when the cavity is at the nominal operating temperature of ~2100 K. Further details may be found in Kim's thesis, Ref. 12.

The microwave system outside the vacuum chamber is shown in Fig. 6. The microwave source is a Hewlett Packard (HP) model 8620 sweep oscillator which drives a Varian model VTX 6186B1 traveling-wave-tube amplifier (TWTA). The power level is adjusted after the TWTA by an attenuator. The power is fed into a circulator and then to the microwave cavity. The power reflected from the cavity is directed by the circulator to a HP model 912A attenuator, a HP model 486A waveguide thermistor mount, a HP model 431B power meter, and a HP model 7004A x-y recorder whose x axis is driven by the sweep oscillator. The waveguide thermistor mount and power meter are the primary standard in the experiment for measuring the microwave power and were calibrated by Test Equipment Services, Inc.[13] To measure the mi-

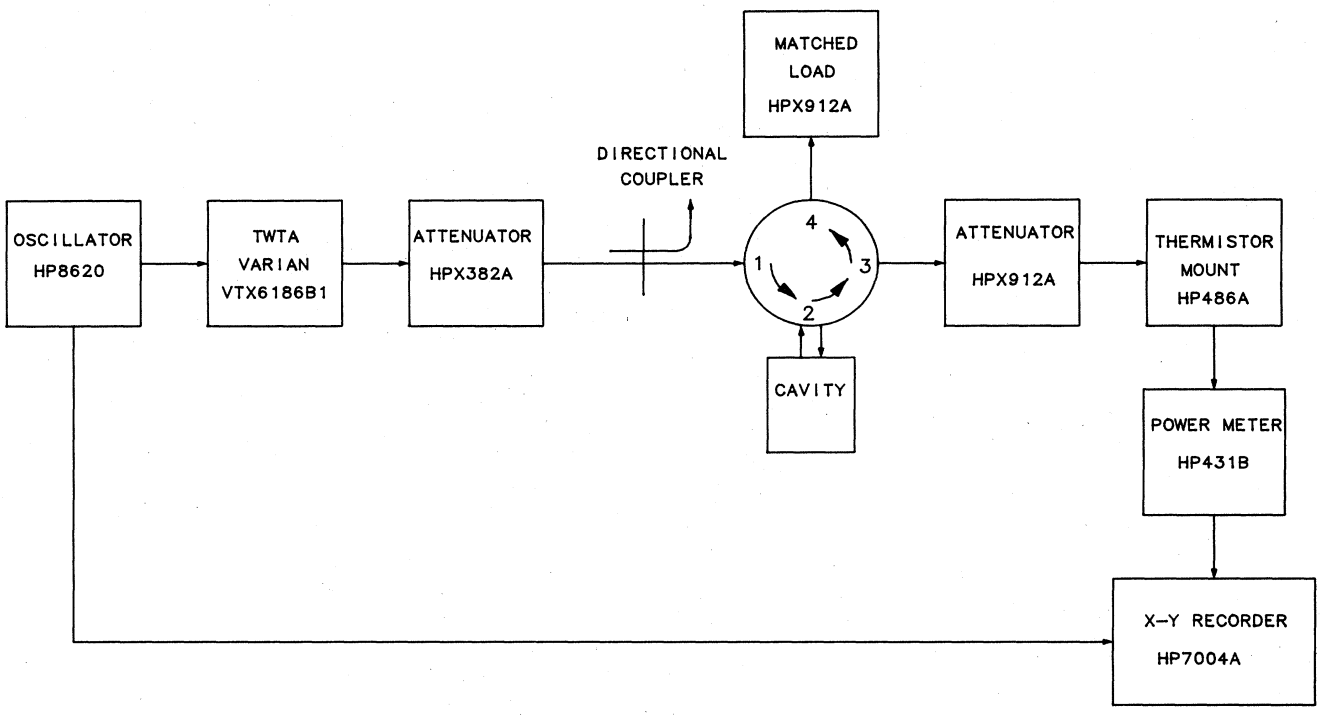

FIG. 6. Microwave system for the frequency-shift measurements.

crowave power incident on the cavity, the waveguide thermistor mount is inserted at the point where the power first enters the circulator. The microwave power diverted by the directional coupler goes to a HP model 382A attenuator, a waveguide to coaxial adaptor, a HP model 423B coaxial low-barrier Schottky detector, and an oscilloscope. A HP model 352 wavemeter is inserted between the attenuator and adaptor.

VI. CAVITY MICROWAVE POWER AND Q

The two quantities necessary to evaluate the field strengths in the cavity are the power delivered to the cavity, P_c, and the internal Q of the cavity, Q_0. Measuring these two quantities is not straightforward as the vacuum part of the waveguide system contains components, some of them fabricated in house, that have higher attenuation and reflection coefficients than the more standard microwave components. As mentioned in Sec. II, the cavity is suspended from two waveguides so the microwaves can be used either in transmission or reflection. Transmission gives by far the better-looking resonance curves, but also involves two nonstandard waveguides. Rather than have to deal with two imperfect waveguides in our analysis for Q_0 and P_c it was found advantageous to block off one waveguide and use a single waveguide in the reflection method. Due to the nature of the hot waveguide and other microwave components inside the vacuum system, the reflected microwave signal has significant undulations in power that are not associated with cavity resonances. These undulations make the use of many standard microwave techniques, such as measuring the positions of voltage minima, difficult and tedious. For this reason, we developed a method which depends just on the measurement of various microwave powers for determining P_c and Q_0. The method takes into account the absorption in the waveguide, but does not take into account reflections caused by reactances which produce undulations. The microwave system is represented by the lumped element circuit shown in Fig. 7(a). See, for example, Chap. 9 of Ref. 14. The cavity mode is portrayed as the series circuit composed of the inductance L, the capacitor C, and the resistance R_s. R_s takes into account Ohmic losses in the cavity walls, radiative losses from small holes in the cavity walls other than the coupling aperture, and dissipation in the plasma. The last loss leads in principle to an R_s that is dependent on n_p. This loss is always less than 1% of the total loss in the cavity, and the dependence of R_s on n_p is neglected. The resonant angular frequency is $\omega=1/(LC)^{1/2}$ and the internal Q is $Q_0=(\omega L)/R_s$. The

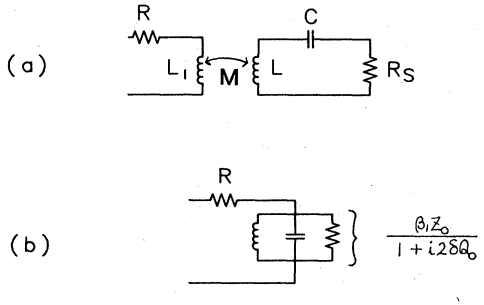

FIG. 7. (a) Equivalent circuit assumed for the cavity and waveguide. (b) The circuit of (a) transformed.

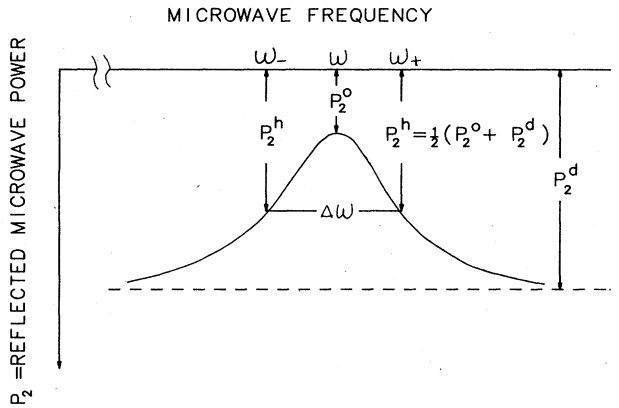

FIG. 8. Model curve of the reflected power P_2 vs the microwave frequency. P_2^d is the detuned reflected power, P_2^h is the reflected power at the half-power points, P_2^0 is the reflected power at resonance, and ω_+ and ω_- are the half-power frequencies.

coupling to the cavity is represented by the mutual inductance M. L_1 is the self-inductance of the coupling aperture, and R accounts for the waveguide losses. It is assumed that the waveguide is driven by a generator matched to the characteristic impedence of the waveguide, Z_0. As shown on page 426 of Ref. 14, if the cavity loop is transformed into the generator loop, and then the self-inductance L_1 of the coupling mechanism is neglected, the circuit of Fig. 7(b) results. The cavity is now represented by a parallel resonant circuit, and the impedance Z_L presented to the microwaves is

$$Z_L = R + \frac{\beta_1 Z_0}{1 + i 2 Q_0 \delta} , \tag{40}$$

where β_1 is the coupling parameter and equal to $(\omega M)^2/(Z_0 R_s)$, δ is the frequency-tuning parameter and equal to $(\omega' - \omega)/\omega'$, and ω' is the microwave frequency. At resonance, $\delta = 0$ and $Z_L = (R + \beta_1 Z_0)$ which is real. Well off resonance δ is large and $Z_L = R$, also real. Let the incidence microwave power be P_1 and the reflected power be P_2. Figure 8 shows P_2 as a function of microwave frequency for the circuit shown in Fig. 7. P_2^d is the detuned reflected power, P_2^0 is the reflected power at resonance, P_2^h is the reflected power and the half-power points for the resonance curve, and $\omega_+ = 2\pi f_+$ and $\omega_- = 2\pi f_-$ are the half-power frequencies. These are the quantities, along with P_c, actually measured. The power absorbed by the cavity at resonance is

$$P_c = (P_1 - P_2^0) \frac{\beta_1 Z_0}{R + \beta_1 Z_0} . \tag{41}$$

P_1 and P_2 are related by $P_2 = |\Gamma|^2 P_1$, where Γ is the voltage-reflection coefficient and equal to $[(Z_L/Z_0) - 1]/[(Z_L/Z_0) + 1]$. With $R' \equiv (R/Z_0)$, it follows that

$$\left[\frac{P_2^d}{P_1} \right]^{1/2} = \pm \frac{R' - 1}{R' + 1} \tag{42}$$

and

$$\left[\frac{P_2^0}{P_1} \right]^{1/2} = \pm \frac{R' + \beta_1 - 1}{R' + \beta_1 + 1} . \tag{43}$$

Equation (42) can be solved for R', and Eq. (43) for $(R' + \beta_1)$. In both cases the sign ambiguity is removed by experimental observations. As the reflected power goes down rather than up when the cavity is tuned to resonance, Eq. (42) leads to

$$R' = \frac{1 - (P_2^d/P_1)^{1/2}}{1 + (P_2^d/P_1)^{1/2}} . \tag{44}$$

The sign ambiguity in Eq. (43) is resolved by measuring the position of a voltage minimum as a function of frequency. This shows the cavity to be undercoupled in the sense that $(R' + \beta_1) < 1$. Thus

$$R' + \beta_1 = \frac{1 - (P_2^0/P_1)^{1/2}}{1 + (P_2^0/P_1)^{1/2}} . \tag{45}$$

Inserting Eqs. (44) and (45) into Eq. (41),

$$P_c = \frac{2(P_1)^{1/2}[(P_1)^{1/2} + (P_2^0)^{1/2}][(P_2^d)^{1/2} - (P_2^0)^{1/2}]}{[(P_1)^{1/2} + (P_2^d)^{1/2}]} . \tag{46}$$

This is the expression used to calculate P_c from measured quantities. When the microwave power is high enough to distort the resonant curves, P_2^0 is taken as the peak of the curve.

Q_0 can be obtained from ω_+ and ω_- as follows. Defining the values of δ at the half power points as $\delta_\pm = (\omega_\pm - \omega)/\omega_\pm$, the equation $P_2 = |\Gamma|^2 P_1$ evaluated at the half-power points gives

$$\frac{P_2^h}{P_1} = \frac{4Q_0^2\delta_\pm^2(R' - 1)^2 + (\beta_1 + R' - 1)^2}{4Q_0^2\delta_\pm^2(R' + 1)^2 + (\beta_1 + R' + 1)^2} . \tag{47}$$

Solving for $\delta_\pm$,

$$\delta_\pm = \pm \frac{1}{2Q_0} \left[\frac{(\beta_1 + R' - 1)^2 P_1 - (\beta_1 + R' + 1)^2 P_2^h}{(R' + 1)^2 P_2^h - (R' - 1)^2 P_1} \right]^{1/2} . \tag{48}$$

Since $\delta_+ = -\delta_-$ and $\omega = \omega_+(1 - \delta_+) = \omega_-(1 - \delta_-) = \omega_-(1 + \delta_+)$, we then have $\omega_+(1 - \delta_+) = \omega_-(1 + \delta_+)$. This last equation can be rearranged to give $\Delta\omega \equiv (\omega_+ - \omega_-) = (\omega_+ + \omega_-)\delta_+$. If δ_+ from Eq. (48) is used and the resulting expression solved for Q_0, then

$$Q_0 = \frac{(\omega_+ + \omega_-)[(P_1)^{1/2} + (P_2^d)^{1/2}]}{2\Delta\omega[(P_1)^{1/2} + (P_2^0)^{1/2}]} . \tag{49}$$

This is the usual expression for Q multiplied by a factor which corrects for the waveguide loss. In measuring the parameters to determine Q_0, low microwave power is used so that the resonant curves are symmetric.

VII. EXPERIMENTAL PROCEDURE AND DATA

After appropriate outgassing of the plasma device, the cavity is brought to the operating temperature. The

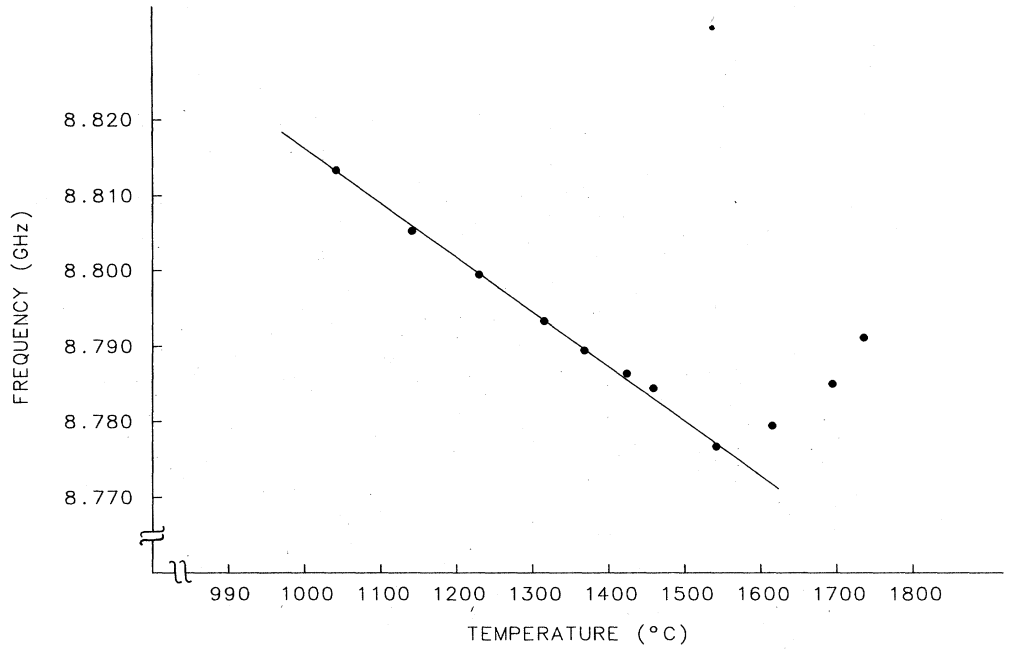

FIG. 9. Frequency of the TM_{010} mode vs the cavity temperature. The alkali oven is cold for these data.

heater power to the alkali oven is then adjusted to give the desired plasma density at low microwave power, n_{p0}. n_{p0} is determined by using Eq. (38) which relates this quantity to f, the resonant frequency of the TM_{010} mode of the filled cavity at low microwave power, and f_0, the resonant frequency of the same mode of the empty cavity. The necessary resonant frequencies are read from resonant curves which are obtained by feeding a voltage proportional to the reflected microwave power into the y axis, and a voltage proportional to frequency into the x axis, of an x-y recorder. The determination of f is straightforward, while the determination of f_0 is complicated by the fact that the cavity at operating temperatures always has plasma in it, even when the alkali oven is cold. This is particularly true after alkali has once been introduced into the cavity. To circumvent this effect, the alkali oven is kept cold and f is measured as a function of $T_w = T_e = T_i$ for temperatures from about 1050 °C up to the operating temperature. Examples of the data are shown in Fig. 9. The linear portion of the curve with negative slope between 1050 °C and 1500 °C is due to a nearly empty cavity which is expanding as the temperature increases and represents accurate values of f_0 for the corresponding temperatures. For temperatures slightly above 1500 °C the curve starts to increase due to the presence of plasma. f_0 for these higher temperatures is determined by extending the straight-line portion of the curve.

With the plasma at the desired density, a series of resonant curves are taken each at a higher power than its predecessor. Tracings of three curves from a series are shown in Fig. 10. The K plasma has $n_{p0} = 2.28 \times 10^{16}$

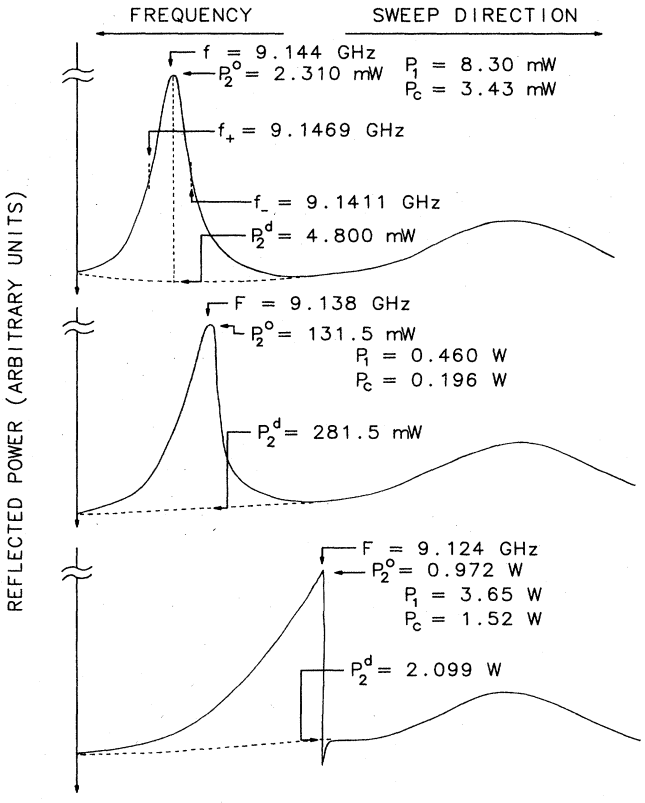

FIG. 10. Tracings of three resonant curves from run No. 2.

m^{-3} and $T_e = 2048$ K. The frequency is swept from high to low and decreases to the right in the graphs. Frequency markers are not shown. Reflected power increases in the downward direction so that the resonant curves appear upright. The vertical power scales are different for the three curves, but the horizontal frequency scales are the same. After the series of curves is recorded on separate sheets of paper, the plasma density is changed sufficiently to move the resonant curve out of the frequency range being swept. Then each curve is put back in the x-y recorder and a background curve taken. In the frequency region of the resonance, this is shown as a dotted curve in Fig. 10. Away from the resonance the background curve and the curve containing the resonance are so close as to be represented by a single line in the figure. This fact allows us to infer that the background curve in the vicinity of the resonance is a proper "baseline" for the resonance curve.

The top curve in Fig. 10 is the low-power curve. It is undistorted by power, quite symmetric, and is used to determine f and Q_0. The parameters f, f_+, f_-, P_2^0, and p_2^d are obtained from this curve as shown in the figure. As explained in Sec. V, P_1 is measured independently and found to be 8.30 mW. Then Eq. (46) is used to give P_c as 3.43 mW and Eq. (49) gives Q_0 as 1824. The bottom two curves have had their peaks shifted downward in frequency. The peaks are now designated by F, and the frequency shift is $(f - F)$. The determinations of P_2^0 and P_2^d are also indicated. The shapes of these curves are distorted by the power because the plasma density changes during the frequency sweep. Far out on the high-frequency wing of the resonance very little power gets into the cavity. Negligible electron heating and plasma-density reduction take place and the resonant curve is similar to the top curve. To the left of the resonant peak, as the frequency continues to move downward, more power gets into the cavity and the density decreases, decreasing the resonant frequency. In effect, the decreasing microwave frequency "pushes" the cavity resonant frequency downward ahead of it. At the peak of the curve, the maximum reduction in density for the fixed amount of incident power being used is obtained. To the right of the resonant peak a further reduction in frequency results in less power to the cavity and causes the resonance to now move up in frequency as the frequency sweep continues to move downward. This accounts for the steep right-hand side of the curves. The right-hand side of the bottom curve is so sharp that x-y recorder overshoot is evident. As would be

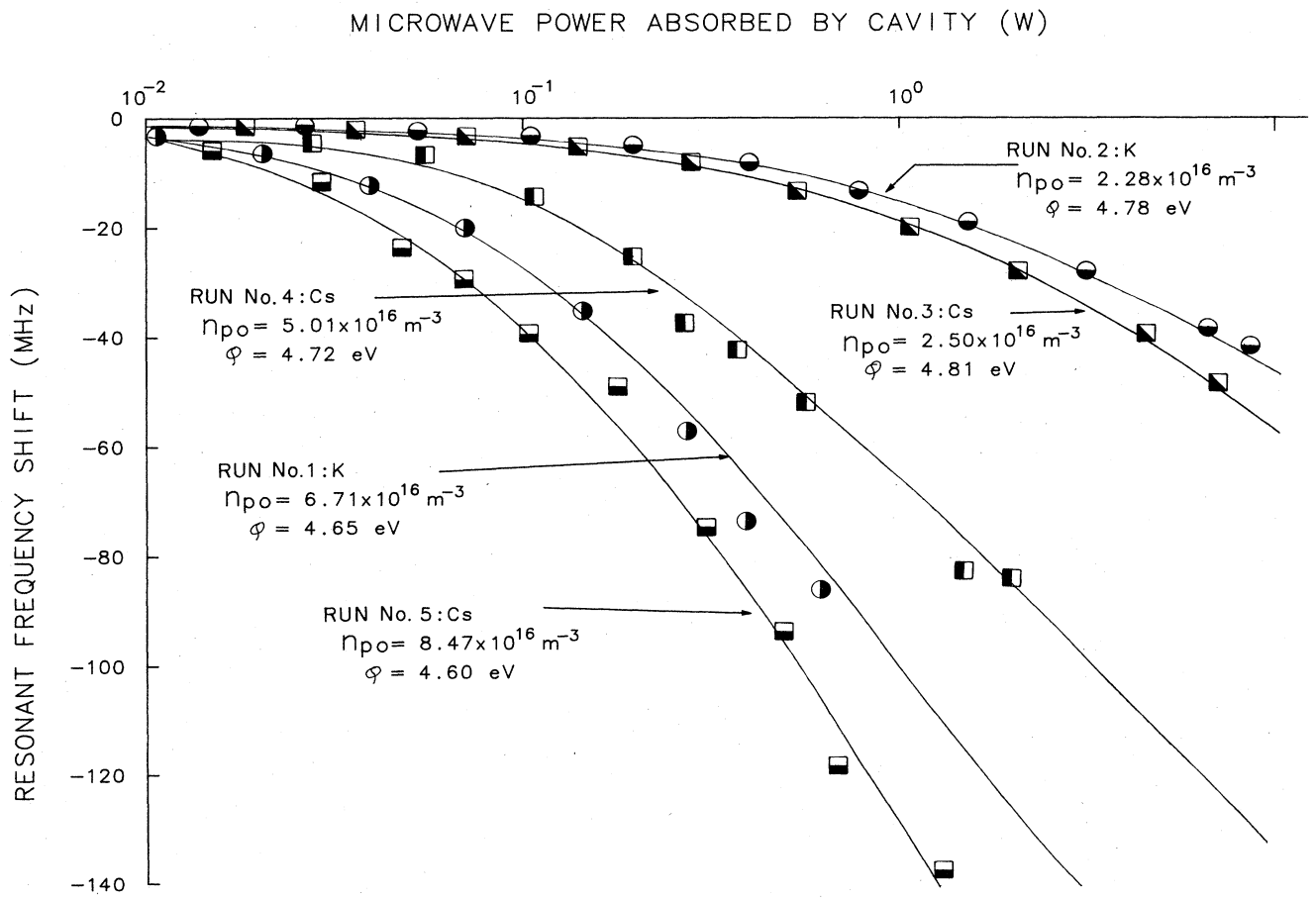

FIG. 11. Frequency shift vs the microwave power absorbed by the cavity for runs No. 1—No. 5. The solid curves are the predictions of the hot-electron theory. The cavity wall temperatures are runs No. 1 and No. 2, 2048 K; run No. 3, 2033 K; run No. 4, 2036 K; and run No. 5, 2037 K.

expected, there is considerable hysteresis in the resonant curve if the frequency is now swept back through the resonance from low to high frequency, the frequency shift being less. In taking data, the frequency was always swept from high to low frequency so as to obtain the maximum frequency shift for the power being used.

At some microwave frequencies and for the highest microwave powers used, the reflected microwave power was modulated at frequencies of from 30 to 60 kHz. This was observed by looking at the demodulated reflected microwave power on a 1-MHz oscilloscope. Frequencies for which this occurred were not used in the data presented. The modulation of the reflected microwave power is probably caused by ion acoustic oscillations of the plasma in the cavity. The density fluctuations associated with the ion acoustic oscillations would change the impedance presented to the waveguide by the cavity, resulting in the modulated reflected microwave signal. We are not reporting on these effects here except to note that for the data analyzed density oscillations in the plasma at frequencies $\lesssim 1$ MHz were not present at sufficient levels to be observed in our oscilloscope.

Due to continual improvements in the apparatus, the last five runs are the most reliable, and for convenience are numbered from 1 to 5. The data for each run consist of from 9 to 11 high-power resonant curves plus one resonant curve at low power. Figure 11 shows the resonant frequency shifts versus the microwave powers absorbed by the cavity for these runs. Runs No. 1 and No. 2 are for a K plasma, and runs No. 3—No. 5 are for a Cs plasma. For each run n_{p0} and T_w are held constant. The densities for the different runs range from 2.28×10^{16} m^{-3} to 8.47×10^{16} m^{-3}, and are given in the figure. The temperature for the runs are all around 2050 K, but the exact values are in the figure caption. The data for each run have been fit by a curve calculated from the hot-electron theory of Sec. IV. The work function φ used for each curve has been adjusted so the curve passes through the points near the middle of the data. For the different curves, the values of φ range from 4.60 to 4.81 eV, and given in the figure.

For the data presented in Fig. 11, the frequency measurements are accurate to ±1 MHz, and the temperature measurements to ±10°C. The latter have been corrected for absorption by the window through which the optical pyrometer is sighted. The random error associated with the measurement of microwave power is estimated to be $\pm5\%$, about the horizontal width of the data point symbols in the figure. Due to calibration uncertainties of the microwave-power-measuring equipment and attenuators, a systematic error of up to $\pm15\%$ may affect all power measurements. The quoted Q's are estimated to be accurate to $\pm10\%$.

VIII. DISCUSSION

The frequency of the TM_{010} mode of a hot cylindrical cavity filled with a surface ionized K or Cs plasma has been measured as a function of microwave power to the cavity. The electric fields and pressures are not high enough for significant ionization of the plasma by electron impact to occur, and microwave excited instabilities have been avoided. It has been found, as shown in Fig. 11, that the resonant frequencies are lowered as the microwave power increases. This implies that either the ponderomotive force has pushed the plasma away from regions of high electric fields, or that the plasma density has been reduced by the microwave fields in some other way. A theory has been developed which assumes that the fields heat the electrons resistively. The plasma equilibrium is then shifted so that the plasma density is decreased while the neutral density is increased. This hot electron theory is portrayed by the solid curves in Fig. 11. Not shown in Fig. 11 are curves calculated from the ponderomotive-force theory. These curves show frequency shifts that are of the order of 2% of those for the hot-electron theory. It is apparent that ponderomotive force effects are not responsible for the frequency shifts.

As explained in Sec. IV, the data for each of the five runs are fitted by a curve generated by the hot-electron theory. The work function φ of the cavity wall is treated as an adjustable parameter for each curve, so that there are five values of the work function used to fit the data. The data for a given run are represented very well by its curve. φ has been adjusted so that the data and curve agree near the middle, but note that there is a range of power of from 100 to 1000 for each curve and agreement is good over the whole power range. Furthermore, the frequency shift versus power data is not represented by simple linear, exponential, or power-law functions. The relationship between frequency and power is complicated and well represented by the hot-electron theory.

To fit the hot-electron theory to all five runs, it is necessary to assign different values of φ to each run. The fitting of the curves is quite sensitive to the value of φ. Two workers might differ by 0.01 eV in the assignment of φ, but it is unlikely that they would differ by as much as 0.02 eV. Thus the differences in the values of φ for runs No. 1, No. 4, and No. 5 are significant, as are the differences between these runs and runs No. 2 and No. 3, while the differences between runs No. 2 and No. 3 are not too significant. It is noteworthy that the values of φ increase as the plasma density decreases, except for runs No. 2 and No. 3 which are quite close together in density. The obvious explanation is that alkali wall coverage is lowering φ at the higher densities. It would be desirable to have quantitative confirmation of this effect. Taylor and Langmuir[15] determined the work function of W partially coated with Cs, but, unfortunately, measurements do not seem to have been made for K and Cs on Re. We do not attribute too much significance to the fact that all our values of φ are below the value of 4.96 eV measured by Wilson.[16] In our measurements there is always some alkali present while Wilson's measurements were made on clean surfaces. Additionally the work function depends sensitively on the crystal structure of the surface, and it is possible our Re plating was not quite complete, or flaked off in isolated spots.

The ionization potentials of the atoms used, 3.89 eV for Cs and 4.34 eV for K, appear exponentially in the theory. The use of both K and Cs is a sensitive check of the theory, and the data of Fig. 11 are fitted well for both al-

kalis. We conclude that the frequency shifts observed are adequately described by the hot-electron theory.

ACKNOWLEDGMENTS

This work was supported by the National Science Foundation.

APPENDIX

A perturbation calculation of the resonant frequency shift of the TM_{010} mode, valid for small values of E and the expansion parameter $\mu=\omega_{p0}^2/\omega_0^2$, was made as a further check on the computer-calculated frequency shift. This calculation is patterned after methods discussed by Hayashi.[17] The starting point is Maxwell's equations (9) and (10). Instead of eliminating E in favor of H, H is eliminated in favor of $E_z=E$ so that

$$r\frac{d^2E}{dr^2}+\frac{dE}{dr}+\frac{\omega^2KrE}{c^2}=0\ , \tag{A1}$$

where c is the velocity of light in a vacuum. With vacuum in the cavity, $K=1$, and this reduces to Bessel's equation. Then the peak electric field in the cavity is $E=AJ_0(\alpha_{01}r/a)$, where J_0 is the zeroth-order Bessel function, and α_{01} is its first zero. The radius of the cavity is a, and the maximum value of E, which is on the cavity axis, is A. The vacuum resonant frequency is $\omega_0=(\alpha_{01}c)/a$.

With plasma present the cold plasma dielectric constant K is given by Eq. (2). Following is an expansion of K in terms of A, the maximum value of E in the cavity and not a function of r, and E, the peak value of the electric field in the cavity and given, for low values of E, by $AJ_0(\alpha_{01}r/a)$. n_{pw}, the plasma density at the cylindrical wall, is a function of A (but not of r) because, as in the computer calculation, the total number of charged plasma particles is required to stay constant. Letting the unperturbed constant plasma density be n_{p0}, the equation governing the value of n_{pw} is the integral of Eq. (7) over the volume of the cavity, which is

$$\int_V n_p(r)d^3x=\int_V n_{pw}\exp[-(e^2E^2)/(8m\omega^2kT_e)]d^3x$$
$$=n_{p0}V\ . \tag{A2}$$

To calculate the dependence of n_{pw} on A, the J_0 Bessel-function dependence of E is used. The latter is a good approximation for low values of E, as the computer calculation indicates that the dependence of E upon r hardly changes as E increases. The exponential in Eq. (A2) is expanded, and the result integrated, yielding

$$n_{p0}=n_{pw}\{1-[DA^2J_1^2(\alpha_{01})]/\omega^2\}\ , \tag{A3}$$

where $D=e^2/(8mkT_e)$. $J_1^2(\alpha_{01})$ arises from

$$h\int_0^a J_0^2(\alpha_{01}r/a)2\pi r\,dr=VJ_1^2(\alpha_{01})\ , \tag{A4}$$

where J_1 is the first-order Bessel function and h is the height of the cavity. Solving for n_{pw} and expanding,

$$n_{pw}=n_{p0}\{1+[DA^2J_1^2(\alpha_{01})]/\omega^2\}\ . \tag{A5}$$

Putting this result in Eq. (8) and expanding the exponential in that equation, K becomes to order A^2 and E^2,

$$K=1-\omega_{p0}^2/\omega^2-[D\omega_{p0}^2A^2J_1^2(\alpha_{01})]/\omega^4$$
$$+(D\omega_{p0}^2E^2)/\omega^4\ . \tag{A6}$$

Expressing ω_{p0} in Eq. (A6) in terms of the dimensionless expansion parameter μ and substituting K into Eq. (A1), there results

$$r\frac{d^2E}{dr^2}+\frac{dE}{dr}+\frac{r}{c^2}[\omega^2-\mu\omega_0^2-\mu\omega_0^2\omega^{-2}DA^2J_1^2(\alpha_{01})]E$$
$$+\mu rDc^{-2}\omega_0^2\omega^{-2}E^3=0\ . \tag{A7}$$

The fields and frequency are now expanded in powers of μ where subscripts indicate the order in the expansion,

$$E=E_0+\mu E_1+\mu^2E_2+\cdots\ , \tag{A8}$$

$$\omega^2=\omega_0^2+\mu\omega_1^2+\mu^2\omega_2^2+\cdots\ , \tag{A9}$$

$$1/\omega^2=1/\omega_0^2-(\mu\omega_1^2)/\omega_0^4$$
$$+\mu^2(\omega_1^4/\omega_0^6-\omega_2^2/\omega_0^4)+\cdots\ , \tag{A10}$$

and

$$E^3=E_0^3+\mu 3E_0^2E_1+\mu^2 3E_0(E_0E_2+E_1^2)+\cdots\ . \tag{A11}$$

Using these expressions in Eq. (A7), and collecting the zeroth-order terms gives

$$r\frac{d^2E_0}{dr^2}+\frac{dE_0}{dr}+r\omega_0^2c^{-2}E_0=0 \tag{A12}$$

with the solution $E_0=AJ_0(\alpha_{01}r/a)$. Collecting the first-order terms gives

$$r\frac{d^2E_1}{dr^2}+\frac{dE_1}{dr}+\omega_0^2rc^{-2}E_1$$
$$=-\frac{r}{c^2}\{[\omega_1^2-\omega_0^2-DA^2J_1^2(\alpha_{01})]E_0+DE_0^3\}\ . \tag{A13}$$

To extract ω_1 from Eq. (A13), E_1 and E_0^3 are expanded in a series of J_0's as

$$E_1=\sum_{i=1}^{\infty}a_iJ_0(\alpha_{0i}r/a) \tag{A14}$$

and

$$E_0^3=A^3J_0^3(\alpha_{0i}r/a)=A^3\sum_{i=1}^{\infty}b_iJ_0(\alpha_{0i}r/a)\ . \tag{A15}$$

The first term in the expansion for E_1 is $a_1J_0(\alpha_{01}r/a)$ and makes the left-hand side of Eq. (A13) zero. Therefore the projection of the right-hand side onto $J_0(\alpha_{01}r/a)$ must be zero. The projection of E_0^3 onto $J_0(\alpha_{01}r/a)$ is the coefficient of the first term of the series in Eq. (A15). This projection is b_1A^3, where

$$b_1=\frac{\int_0^a J_0^4(\alpha_{01}r/a)r\,dr}{\int_0^a J_0^2(\alpha_{01}r/a)r\,dr}=0.5658\ . \tag{A16}$$

Then equating the total coefficient of $J_0(\alpha_{01}r/a)$ on the

right-hand side to zero gives

$$\omega_1^2=\omega_0^2+[J_1^2(\alpha_{01})-b_1]A^2D\ . \tag{A17}$$

To first order, the desired eigenfrequency ω of Eq. (A1) is given by

$$\omega^2=\omega_0^2+\mu\omega_1^2$$
$$=\omega_0^2+\omega_{p0}^2+\omega_{p0}^2\omega_0^{-2}DA^2[J_1^2(\alpha_{01})-b_1]\ . \tag{A18}$$

The expression relating A to the cavity power P_c and the cavity Q_0 is

$$A^2=\frac{2\omega P_c Q_0}{\epsilon_0\pi a^2 h(\omega^2-\omega_{p0}^2)J_1^2(\alpha_{01})}\ , \tag{A19}$$

where the variation of the dielectric constant K over the cavity volume is neglected. Inserting this into Eq. (A18),

$$\omega^2=\omega_0^2+\omega_{p0}^2+\frac{2\omega\omega_{p0}^2DP_cQ_0[J_1^2(\alpha_{01})-b_1]}{\epsilon_0\pi a^2 h\omega_0^2(\omega^2-\omega_{p0}^2)J_1^2(\alpha_{01})}\ . \tag{A20}$$

For a given P_c, Q_0, and ω_{p0}, ω is obtained by using the solve routine of a Hewlett Packard 15C calculator.

The predictions of Eq. (A20) have been compared to the computer calculation for a cavity with a Q of $Q_0=1500$, a plasma with $T_e=2100$ K, and densities of from 2×10^{16} to 1×10^{17} m^{-3}. The perturbation calculation gives frequency shifts that are from 10% to 25% higher than the computer calculation for microwave powers ranging from 0.14 to 14 W. As would be expected, the agreement is best (10%) for low plasma density and low microwave power. The agreement is close enough to give us reasonable confidence in the computer calculation and reinforce our belief that the ponderomotive force is not responsible for the bulk of the frequency shifts.

*Present address: AT&T Bell Laboratories, Holmdel, NJ 07733.

[1]I. L. Klavan, D. M. Cox, H. H. Brown, Jr., and B. Bederson, Phys. Rev. Lett. **28**, 1254 (1972).

[2]D. M. Cox, H. H. Brown, Jr., I. K. Klavan, and B. Bederson, Phys. Rev. A **10**, 1409 (1974).

[3]D. M. Cox, H. H. Brown, Jr., L. Schumann, F. Murray, and B. Bederson, Phys. Rev. A **10**, 1711 (1974).

[4]D. Taggart, L. Schumann, and H. H. Brown, Jr., Phys. Fluids **24**, 1180 (1981).

[5]H. Motz and C. J. H. Watson, in *Advances in Electronic and Electron Physics,* edited by L. Marton (Academic, New York, 1967), Vol. XXIII, p. 153.

[6]H. Motz, in Proceedings of the Fifth International Conference on Ionization Phenomena in Gases, Munich, 1961 (unpublished), p. 1484.

[7]H. Motz, in *Numerical Solutions of Ordinary and Partial Differential Equations,* edited by L. Fox (Pergamon, New York, 1962), p. 469.

[8]B. W. Arden and K. N. Astill, *Numerical Algorithms: Origins and Applications* (Addison-Wesley, New York, 1970), p. 201.

[9]R. W. Motley, *Q Machines* (Academic, New York, 1975), p. 10.

[10]I. P. Shkarofsky, T. W. Johnston, and M. P. Bachynski, *The Particle Kinetics of Plasmas* (Addison-Wesley, Reading, Mass., 1966).

[11]A. R. Meyer, Trans. Inst. Metal Finishing **46**, 209 (1968).

[12]Kwang S. Kim, thesis (University Microfilms International, Ann Arbor, Michigan), Order No. 83-13914.

[13]Test Equipment Service Inc., South Plainfield, N.J., Report No. 10241; Report No. 10242.

[14]E. L. Ginzton, *Microwave Measurements* (McGraw-Hill, New York, 1957).

[15]J. B. Taylor and I. Langmuir, Phys. Rev. **44**, 423 (1933).

[16]R. G. Wilson, J. Appl. Phys. **37**, 3170 (1966).

[17]C. Hayashi, *Nonlinear Oscillations in Physical Systems* (McGraw-Hill, New York, 1964).